SUPPLEMENTAL DATA

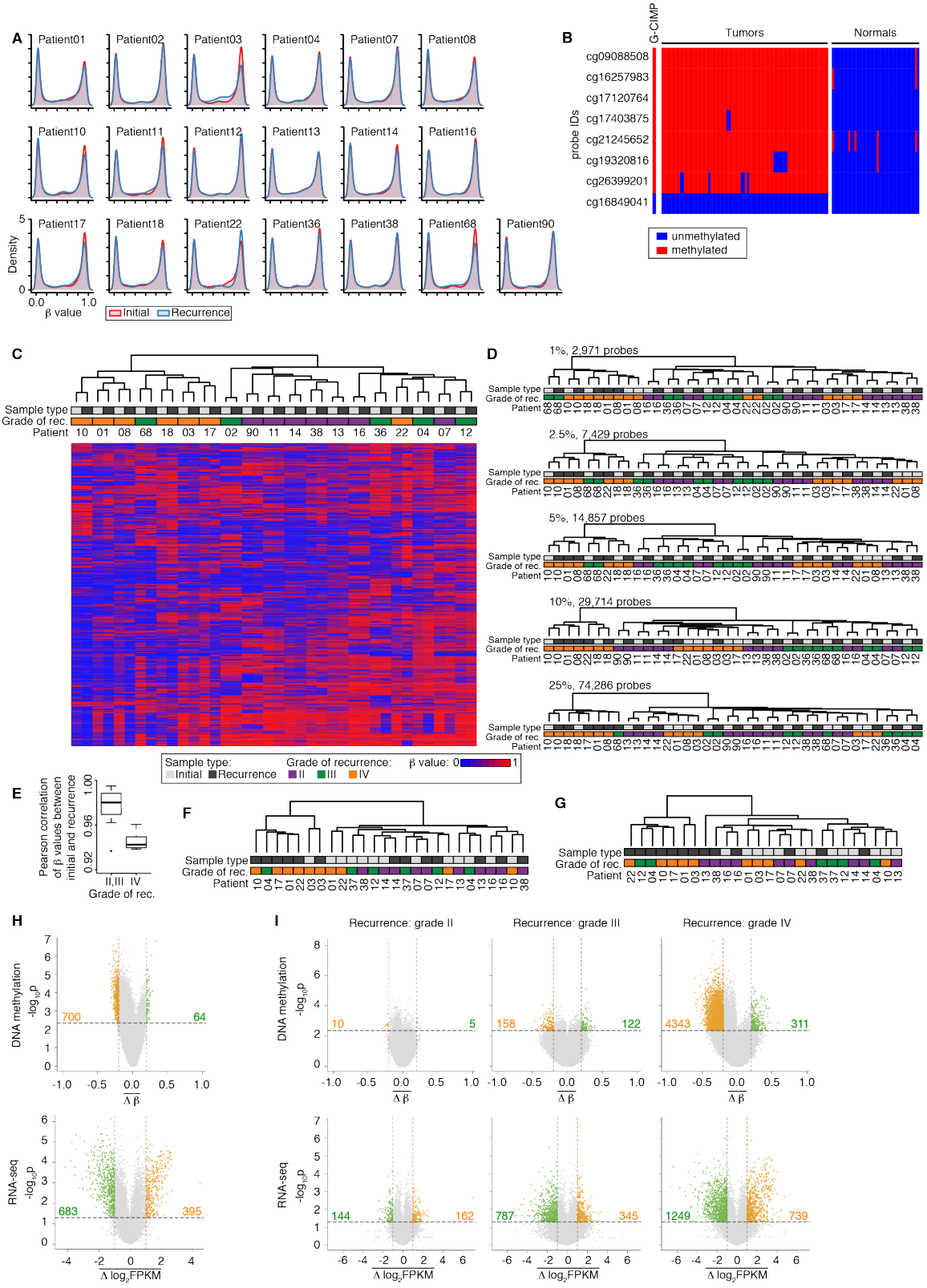

Figure S1, related to Figure 1

(A) Density plots of background corrected and normalized beta values in each initial and recurrent tumor.

(B) Confirmation of the presence of the glioma CpG island methylator phenotype (G-CIMP) in all initial tumors and maintenance of G-CIMP at recurrence (tumor n=70). G-CIMP is absent from all normal brain tissues examined (normal brain n=38).

(C) Unsupervised hierarchical clustering of the top 0.5% most variable CpG sites and heatmap of beta values.

(D) Unsupervised hierarchical clustering of the most variable CpG sites at intermediate (top 1%, 2.5%, 5%, 10%, 25%) cutoffs.

(E) Boxplot summarizing Pearson correlations of beta values between initial and recurrent tumors for each patient, grouped by the grade of the recurrent tumor, show decreased correlations in patients that recur as GBM. The box encompasses data points between the first and third quartiles, with a horizontal line indicating the median value. Whiskers extend to 1.5 x interquartile range, and any data points beyond that range are shown as individual dots.

(F, G), Unsupervised hierarchical clustering of the top 1% (F) or top 50% (G) most variably expressed genes across the cohort.

(H) The methylation change (top) and expression change (bottom) from initial low-grade tumor to recurrence at each CpG site (top) and gene (bottom), averaged across all patients in the cohort. Colored dots represent CpG sites (top) and genes (bottom) that show significant changes at recurrence. The number of significant CpG sites (top) and genes (bottom) are provided in each quadrant.

(I) Methylation (top) and expression (bottom) changes from initial to recurrent tumor, subdivided by the grade of the recurrent tumor.

Table S1, related to Figure 1: Summary of the data types acquired, clinical features, treatment history and molecular features of each tumor in the cohort

Provided as an Excel file.

Table S2, related to Figure 1: QC of all sequencing datasets

Provided as an Excel file.

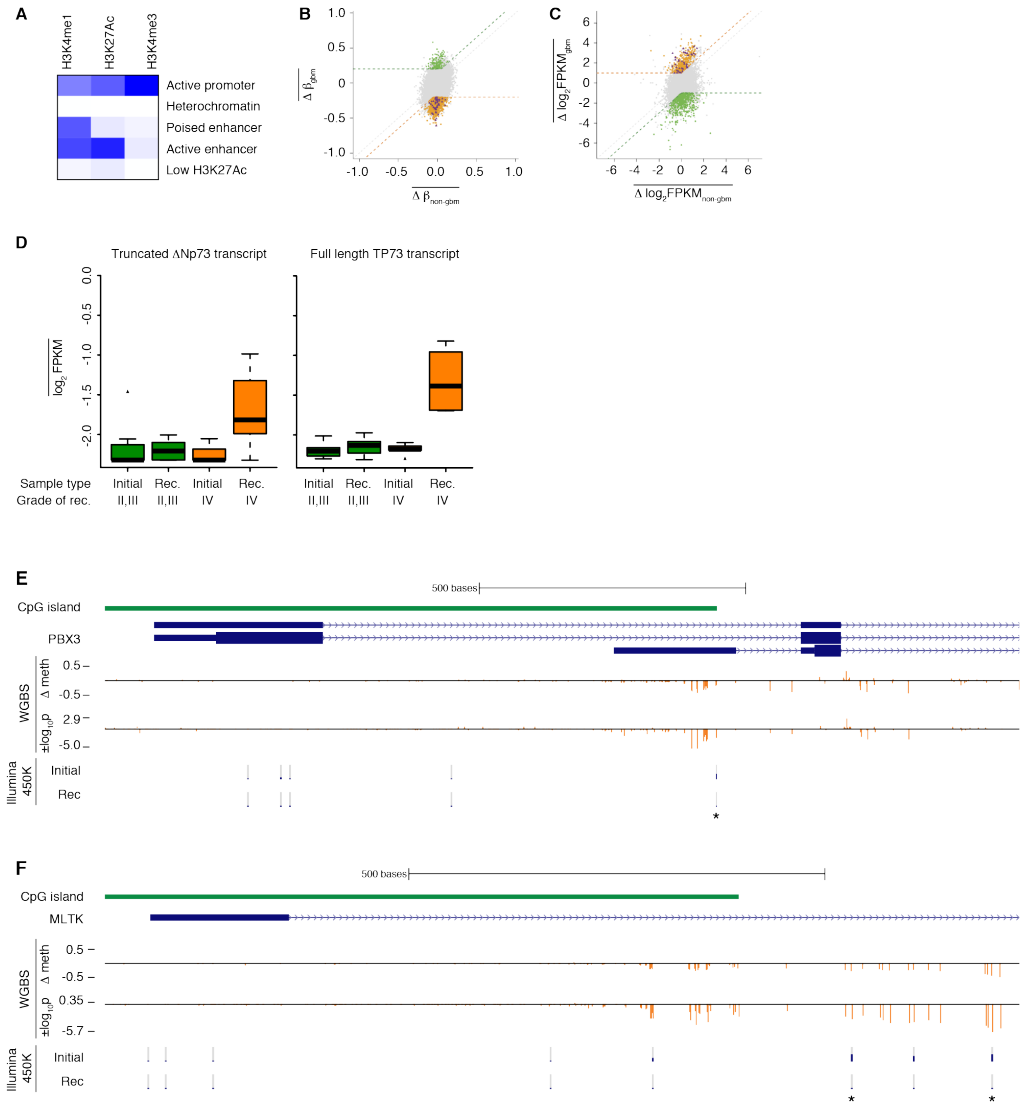

Figure S2, related to Figure 2

(A) Chromatin state outputs from ChromHMM applied to ChIP-seq for H3K4me1, H3K4me3, and H3K27ac. The intensity of the color in each box indicates the probability that a particular mark is present in each state.

(B, C) Scatterplots show how the average change from initial to recurrent tumor in methylation (B) and expression (C) for each CpG site or gene differs between patients that recur as GBM (y-axis) and those that recur at grades II or III (x-axis). Purple

triangles highlight genes that become hypomethylated at promoter CpGs (B) and over-expressed (C) during malignant progression to GBM (see Supplemental Experimental Procedures).

(D) Boxplot of log_2FPKM of all full-length TP73 (ENST00000346387.4, ENST00000354437.4, ENST00000357733.3, ENST00000378295.4, ENST00000603362.1, ENST00000604074.1, ENST00000604479.1) and truncated ΔNp73 (ENST00000378280.1, ENST00000378285.1, ENST00000378288.4) transcripts, averaged per patient. Both transcripts are uniquely expressed in grade IV recurrences. The box encompasses data points between the first and third quartiles, with a horizontal line indicating the median value. Whiskers extend to 1.5 x interquartile range, and any data points beyond that range are shown as individual dots.

(E, F) WGBS data surrounding CpG sites within the promoter regions of PBX3 (E) and MLTK (F) that were hypomethylated specifically upon recurrence as GBM based on Illumina 450K data. An asterisk marks the CpG sites identified as hypomethylated on the array. Both genes show local regions of hypomethylation in the WGBS data and were upregulated upon recurrence based on transcriptome sequencing. From top to bottom, tracks represent: CpG island; gene transcripts; change in methylation level from initial to recurrent tumor by WGBS; statistical significance of the WGBS methylation changes, where positive values indicate hypermethylation at recurrence and negative values indicate hypomethylation; methylation levels from Illumina 450K array in Patient01 at the CpG sites assayed on the array.

Table S3, related to Figure 2: Probes used for each analysis and gene annotations

Provided as an Excel file.

Table S4, related to Figure 2: GO enrichment results

Provided as an Excel file.

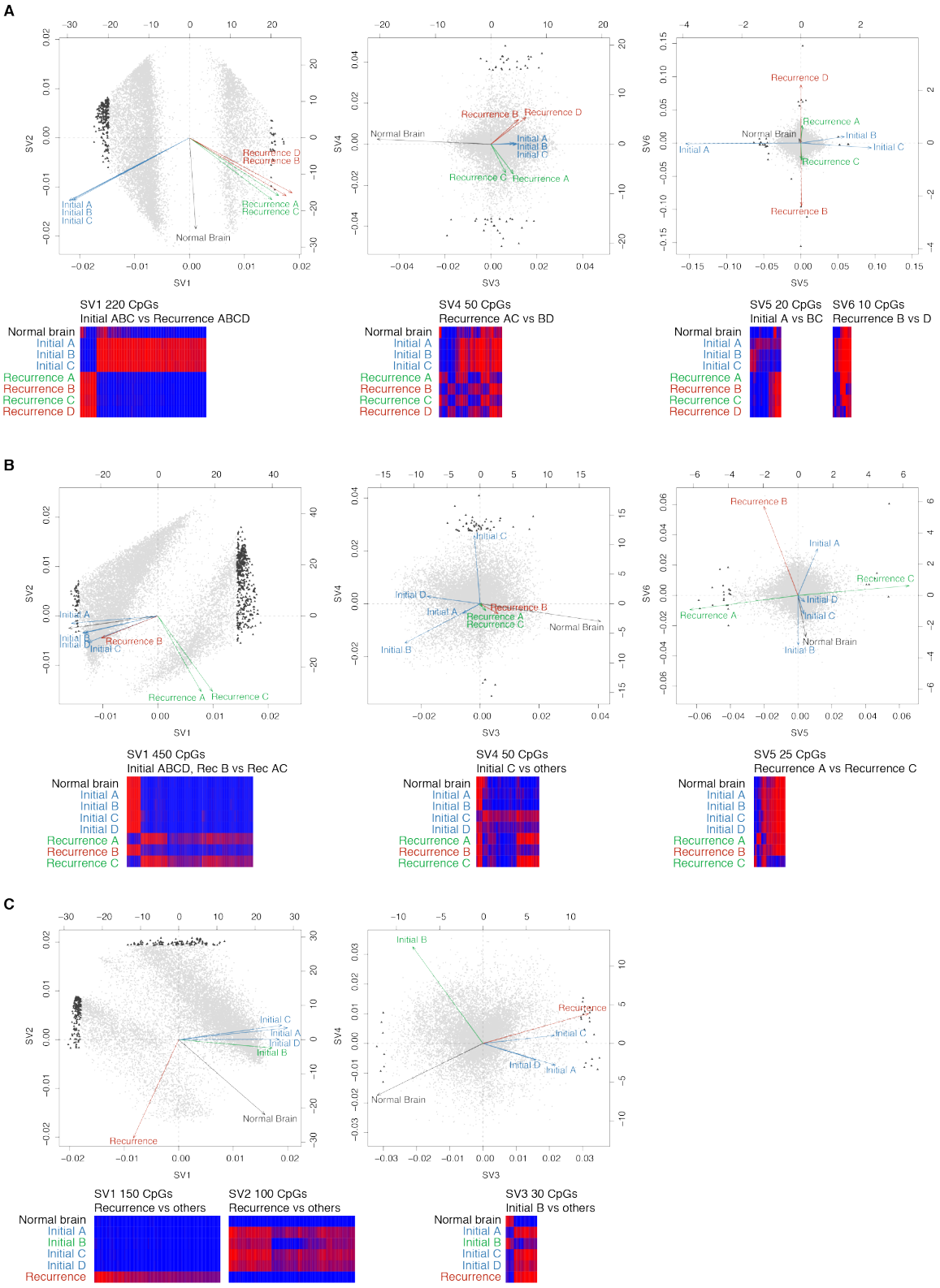
A
SV1
SV2
SV3
SV4
SV5
SV6
Initial A
Initial B
Initial C
Recurrence A
Recurrence B
Recurrence C
Recurrence D
Normal Brain
SV1 220 CpGs
Initial ABC vs Recurrence ABCD
SV4 50 CpGs
Recurrence AC vs BD
SV5 20 CpGs
Initial A vs BC
SV6 10 CpGs
Recurrence B vs D
Normal brain
B
SV1 450 CpGs
Initial ABCD, Rec B vs Rec AC
SV4 50 CpGs
Initial C vs others
SV5 25 CpGs
Recurrence A vs Recurrence C
Initial D
C
Recurrence
SV1 150 CpGs
Recurrence vs others
SV2 100 CpGs
Recurrence vs others
SV3 30 CpGs
Initial B vs others

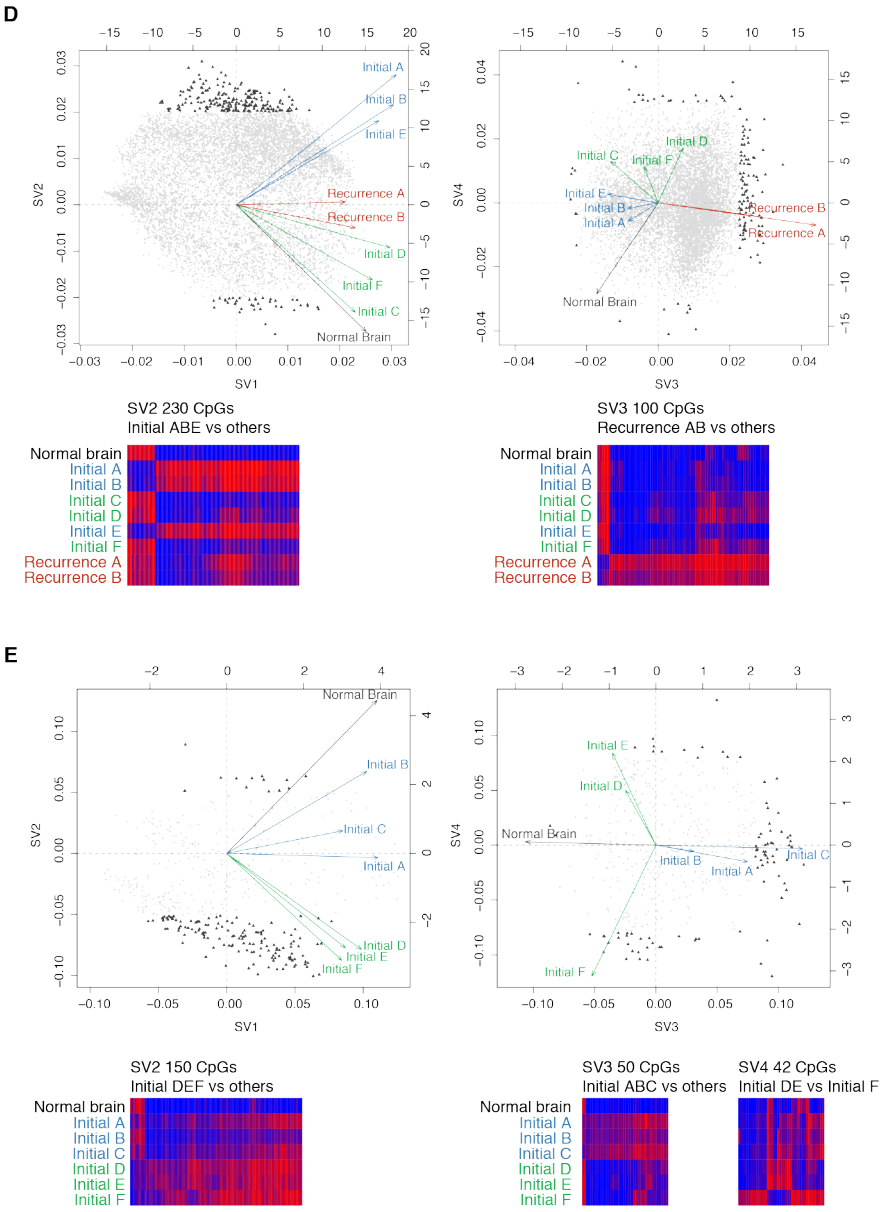

Figure S3, related to Figure 3

(A-E) Singular value decomposition biplots show the probes involved in separating tumor samples for Patient17 (A), Patient01 (B), Patient18 (C), Patient90 (D) and Patient49 (E). Each probe used to build the phyloepigenetic tree is plotted (grey dots).

The most highly weighted probes for each selected SV are highlighted as black triangles. Below each biplot, a heatmap shows the beta values at the most highly weighted probes.

Table S5, related to Figure 3: Somatic mutations used to build phylogenetic trees

Provided as an Excel file.

Table S6, related to Figure 3: Intra- and inter-patient gene-level convergence

Provided as an Excel file.

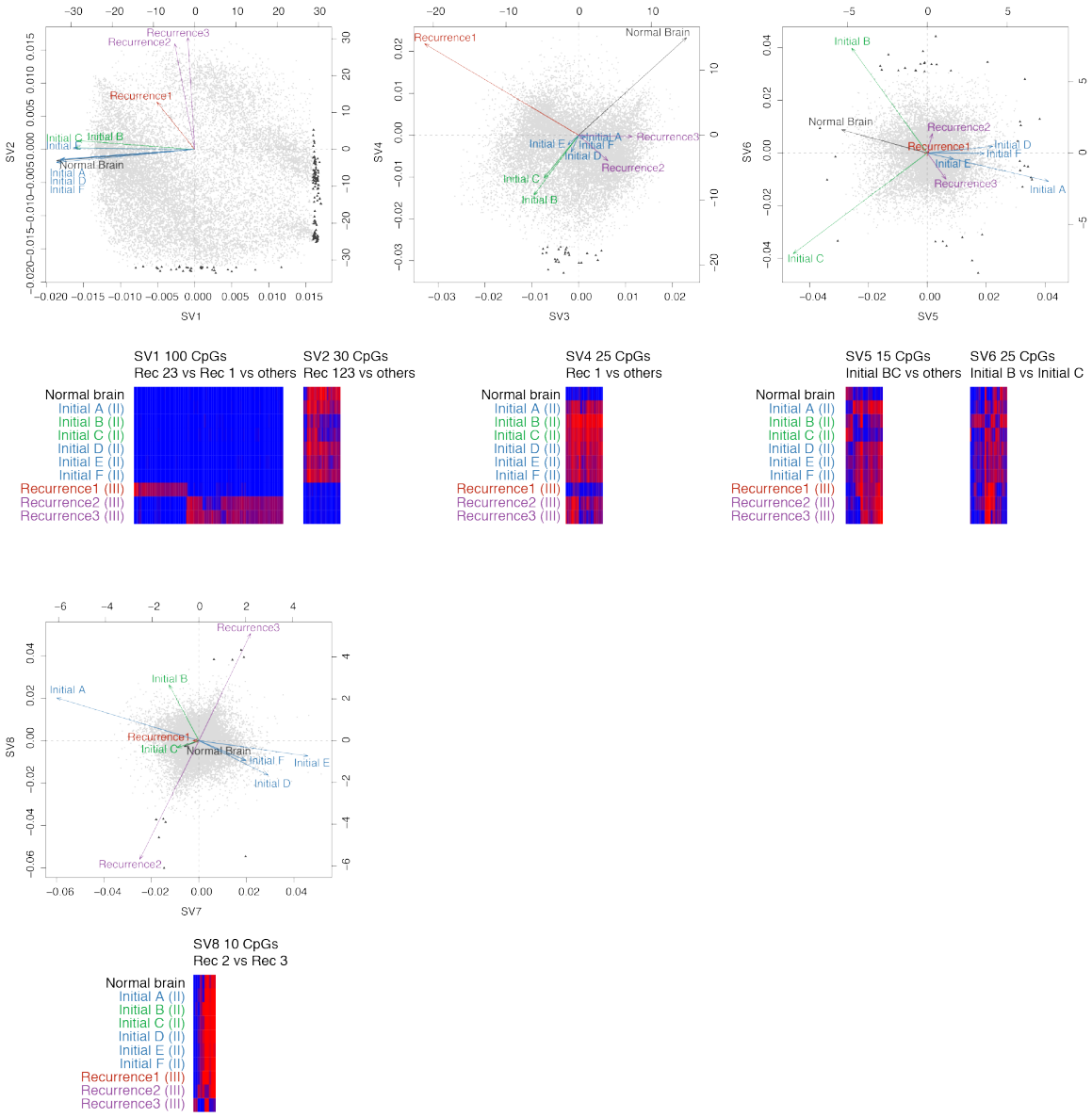

Figure S4, related to Figure 4

Singular value decomposition biplots show the probes involved in separating tumor samples for Patient04. Each probe used to build the phyloepigenetic tree is plotted (grey dots). The most highly weighted probes for each selected SV are highlighted as black triangles. Below each biplot, a heatmap shows the beta values at the most highly weighted probes.

SUPPLEMENTAL EXPERIMENTAL PROCEDURES

Sample acquisition

We collected tissue from patients who underwent multiple surgeries for *IDH1*-mutant astrocytic tumors (1p19q intact) with available flash frozen tissue. All initial and recurrent tumor samples were collected during surgical resection and were snap frozen in liquid nitrogen and stored at -80° C. In cases where more than one sample from a tumor was investigated, those samples were independent, geographically distinct pieces derived from multiple time points during a single surgery. Patient-matched normal samples were peripheral blood mononuclear cells or muscle tissue. Samples were obtained from the Neurosurgery Tissue Bank at the University of California San Francisco (UCSF). Sample use was approved by the Committee on Human Research at UCSF, and research was approved by the institutional review board (IRB) at UCSF. Additional samples were obtained from Erasmus Medical Center with the approval of the Medical Ethics Committee at Erasmus Medical Center Rotterdam and the OncoNeuroTheque tissue bank at Groupe Hospitalier Pitié-Salpêtrière with the approval of the Ethics Committee. All patients provided informed written consent.

Normal brain tissues were acquired from post-mortem human fetal neural tissues (obtained from two cases of twin nonsyndrome fetuses whose deaths were attributed to environmental/placental etiology) and adult insula normal brain (obtained from an autopsy of a case whose death was not related to brain malignancy). Tissues were obtained with written consent according to Partner's Healthcare/Brigham and Women's Hospital IRB and UCSF IRB guidelines. Data from additional fetal and adult normal

brain tissue were obtained from previously published datasets (Kleinman et al., 2014) and publicly available data (CopyNumber450k R package).

DNA and RNA isolation

Genomic DNA was isolated by PCI extraction. Tissues were digested with 1mg/ml proteinase K in lysis buffer (50mM Tris, pH 8.0, 1mM EDTA pH 8.0, 0.5% SDS) overnight at 55°C. After RNase treatment, DNA was phenol/chloroform extracted, precipitated with ethanol and resuspended in TE. RNA was isolated with Trizol (Invitrogen, Carlsbad, CA, USA) according to manufacturer's instruction.

Illumina 450K DNA methylation analysis

Genomic DNA was bisulfite converted using the EZ DNA Methylation Kit (Zymo Research) and processed on Infinium HumanMethylation450 bead arrays (Illumina Inc.) according to the manufacturer's protocol. Probe-level signals for individual CpG sites were subject to both background and global dye-bias correction (Triche et al., 2013). Probes that map to regions with known germline polymorphisms (Illumina supplementary SNP list v1.2, downloaded Sept. 3, 2013), to multiple genomic loci (Price et al., 2013), or to either sex chromosome were filtered out. 297,342 probes remained following filtering. The glioma CpG island methylator phenotype (G-CIMP) was confirmed in all tumors profiled here by examining methylation levels at CpGs adjacent to eight previously defined markers (*ANKRD43*, *HFE*, *MAL*, *DOCK5*, *LGALS3*, *FAS-1*, *FAS-2*, *RHOF*) (Noushmehr et al., 2010). To determine common and specific methylation profiles in the paired initial and recurrent tumors, we performed two-way

unsupervised hierarchical clustering using Euclidean distance and Ward linkage on the most variable CpG sites across the cohort, with variability ranked by standard deviation (0.5% cutoff = 1,486 CpGs; 50% cutoff = 148,572 CpGs).

For all subsequent statistical analyses, beta values for individual CpG sites were made more Gaussian using the logit-transformation. We subtracted the transformed beta values between patient-matched recurrent and initial tumors and used Limma (Smyth, 2004), an empirical Bayes approach utilizing a moderated t-statistic, to test for significant differences in individual CpG sites between the group of patients that recurred as GBM and the group that did not. Differentially methylated CpGs were defined as those with both a nominal p value < 0.05 and an average methylation change upon recurrence ≤ -0.2 or ≥ 0.2. The same empirical Bayes approach was also used to compare methylation differences between the GBM and non-GBM groups. Hypomethylated CpGs were defined as those with both a nominal adjusted p value < 0.05 and an average methylation change upon recurrence as GBM ≤ -0.2 and a difference of the average change between the GBM and non-GBM group of -0.15. Genes associated with the promoter of these GBM-specific hypomethylated CpGs that were also over-expressed upon recurrence as GBM were subject to functional enrichment with clusterProfiler (Yu et al., 2012) against a background of all genes that have methylation probes in their promoter. Here, we defined promoters as 1.5kb upstream of the transcriptional start site (TSS) and 1kb downstream of the TSS.

Age-related methylation

We used Limma to test for the differential methylation between 33 fetal and 8 adult brain tissues. We selected probes having both a nominal adjusted p value (derived from the previous analysis) < 0.05 and an average methylation change upon aging ≥ 0.2.

Gene ontology and enrichment analysis

For all gene ontology analysis, we used the clusterProfiler R package (Yu et al., 2012). In the analysis of methylation changes in annotated promoters, the genes that have methylation probes in their promoters were used as a background. For the analysis of methylation changes in the ChIP-seq-defined enhancer and promoter regions, the genes that have been identified within any regulatory element (everything outside heterochromatin) regions were used as a background. For the enhancer enrichment analysis, we counted probes with genomic coordinates within a region defined as an active enhancer in any of the normal brain or primary GBM samples, and then permuted the probe IDs 10,000 times.

ChIP-seq

Histone ChIP-seq and quality control were performed on four primary GBM frozen tissue samples as previously described (Nagarajan et al., 2014). Briefly, histones marked with H3K4me3 (Cell signaling #9751), H3K4me1 (Diagenode #pAb-037-050), and H3K27Ac (Active Motif #39133), were immunoprecipitated using Sepharose beads coated in protein A/G, and then DNA purified. Pre-aligned ChIP-Seq data of the same histone modifications was downloaded for adult Inferior Temporal Lobe, Hippocampus Middle,

Mid Frontal Lobe, Cingulate Gyrus, and Anterior Caudate from the Human Epigenome Atlas (http://www.genboree.org/epigenomeatlas/multiGridViewerPublic.rhtml).

Genome-wide active promoter and enhancer states were generated from the aligned primary GBM and adult normal brain ChIP-seq data using ChromHMM v1.03 (Ernst et al., 2011). The default parameters were used to binarize the bed files (chromHMM.jar binarizeBed), and the following parameters were used to learn the HMM Model: -xmx3g chromHMM.jar LearnModel 5 hg19. The hidden state showing co-occurrence of high H3K4me3 and H3K27ac marks was assigned as an 'Active Promoter.' Similarly, the state showing co-occurrence of high H3K4me1 and H3K27ac but no H3K4me3 was assigned as an 'Active Enhancer.'

Whole genome shotgun bisulfite sequencing

One to 5μg of genomic DNA was sonicated to an approximate size range of 200–400 bp. DNA was quantified by fluorescent incorporation (Qubit, Invitrogen). Sonicated DNA was subjected to end-repair and phosphorylation with NEBNextTM or Illumina Sample Prep Kit reagents and addition of an 'A' base to the 3′ end. Methylated adapters were ligated and size selection was performed to remove excess free adaptors. The ligated DNA was quantified by Qubit, and 100ng DNA was used for bisulfite conversion. Unmethylated lambda-phage DNA (NEB) ligated with methylated adaptor was used as an internal control for assessing the rate of bisulfite conversion. The ratio of target library to lambda was 1600:1. The methylated adapter-ligated DNA fragments were subject to bisulfite conversion with Qiagen's Epitect Bisulfite Kit (FFPE Tissue Samples Protocol).

Cleanup of the bisulfite-converted DNA was performed, followed by a second round of bisulfite conversion. Enrichment of adaptor-ligated DNA fragments was accomplished by dividing the template into five aliquots followed by eight cycles of PCR with adaptor primers. Post-PCR size-selection of the PCR products from the five reactions was achieved by PAGE gel. Libraries were subject to 100bp paired-end sequencing on Illumina instrumentation.

Individual sequencing lanes were chastity filtered, deduplicated, trimmed of low quality bases and adapter sequence (TrimGalore, http://www.bioinformatics.babraham.ac.uk/projects/trim_galore/) and aligned to hg19 with Bismark v0.10.1 (Krueger and Andrews, 2011). All lanes sequenced from a single library were merged and deduplicated. Methylation information was extracted using Bismark. The posterior distribution of methylation level at each CpG location was obtained using a binomial likelihood and an uninformative beta prior, where the likelihood gives the probability of finding the observed number of methylated cytosine among the total number of reads covering the base. To compute differential methylation between matched samples, the resulting posterior distribution of methylation at each CpG site from the initial tumor was used to compute the beta-binomial posterior predictive distribution and the p value for observing a given number of methylated cytosine at the corresponding site in the recurrence.

Transcriptome sequencing analysis

Strand-specific transcriptome sequencing libraries were prepared as previously described

(Johnson et al., 2014). All transcriptome sequencing data from initial and recurrent tumor pairs were aligned with TopHat (v2.0.12) (Trapnell et al., 2009) to the hg19 reference genome using a GENCODE transcriptome-guided aligment; the following parameters were used: --transcriptome-index=hg19_GencodeCompV19 --library-type fr-firststrand. The aligned data were then processed through custom quality-control scripts to remove unmapped, improperly-matched, multi-mapping, and chimeric reads, as well as accumulation in non-assembled chromosomes. To estimate transcript abundance, aligned data were processed with the cuffnorm and cuffquant commands from the Cufflinks package (v2.2.2) (Trapnell et al., 2010) against a Gencode reference transcriptome (downloaded from UCSC genome browser on 02/03/2014) that has its IDs already linked with official gene symbols. The cuffquant program was run with parameters --max-bundle-frags 50000000 -b hg19.fa --library-type fr-firststrand; the cuffnorm program had the following parameters --compatible-hits-norm --library-type fr-firststrand.

For all subsequent statistical analyses, FPKM estimates for individual genes were made more Gaussian using a log2-transformation. We subtracted the transformed FPKM estimates between patient-matched recurrent and initial tumors and used Limma to test for significant differences among individual genes within the group of patients that recurred as GBM and the group that did not. Differentially expressed genes were defined as those with both a nominal p value < 0.05 and an average log 2-fold change upon recurrence ≤ -1 or ≥ 1. Limma was again used to compare methylation differences between the GBM and non-GBM groups. Upregulated genes were defined as those with both a nominal p value < 0.05 and an average log 2-fold change upon recurrence as GBM

≥ 1 and a difference of the average change between the GBM and non-GBM group of at least 1.

P value adjustment

Statistical tests for assessing significant differences in gene expression and methylation status were performed independently. The varying number of tests performed (~300k for methylation and ~25k for expression), makes it difficult to directly compare the resulting p values. While Storey's false discovery rate controlling for multiple-testing corrections are standard (Storey and Tibshirani, 2003), our data show bimodal distribution of the RNA-seq analysis p values and do not satisfy the assumptions required to apply the method, resulting in incorrect estimation of the number of genes in the null distribution. Thus, we chose our p value cutoffs by identifying the value at which we would identify an equal number of false positives if all the test cases satisfied a null hypothesis and the p values had a uniform distribution. Specifically, by using a .05 cut-off in the expression data, under our simplistic assumptions, to identify the same number of false positives in the methylation data, we would need to use a cutoff $p_{adjusted-methylation} = p_{methylation} * (N_{450k\ probes} / N_{genes})$. Our use of p values here is primarily to rank all probes and genes in our study and follow-up by selecting only those with the most consistent difference.

Identifying discriminative probes by Singular Value Decomposition

The singular value decomposition (SVD) starts with a mean-centered p x n data matrix $\boldsymbol{X}$, where the rows are probes and the columns are samples from a patient. A rank-k approximation of $\boldsymbol{X}$ is obtained from the SVD of $\boldsymbol{X}$ as $\boldsymbol{X_k = UDV^T}$, where $\boldsymbol{U}$ contains the

first k left singular vectors as columns, $\boldsymbol{V}$ contains the first k right singular vectors as columns, and $\boldsymbol{D}$ is a diagonal matrix of the first k singular values. We can rewrite $\boldsymbol{X_k}$ as $\boldsymbol{X_k = (UD^a)\,(D^{1-a}\,V^T) = GH}$, where $\boldsymbol{a}$ determines the scaling of the probes and samples. A biplot uses k=2 and plots the rows of $\boldsymbol{G}$ as points and the columns of $\boldsymbol{H}$ as arrows. For the purpose of performing PCA on samples in the probe space, we used the parameter $a = 0$. The axes at the bottom and left of the biplot are the coordinate axes for the probes while the axes at the top and right of the biplot are the coordinate axes for the samples, allowing us to simultaneously represent both the separation of the samples and the magnitude of each probe contributing towards that separation.

Analysis of gene-level convergence within each patient

We compiled lists of genes with mutations and methylation changes that were present in at least one but not all pieces of tumor from a given patient (excluding hypermutated cases). We enriched those lists for functional events by counting only non-silent mutations and methylation changes in promoter regions. We then used Limma to determine if the methylation levels among the samples with a particular mutation were similar to each other and different from the methylation levels of those samples without the mutation – thus determining if the samples without the mutation had different methylation levels than the samples with the mutation. Table S6 presents the 3 genes (4 CpG sites) for which the absolute value of the t-statistic was greater than 3.5.

Analysis of gene-level convergence among the patient cohort

On a patient level, we identified all genes with non-silent mutations and all genes with

promoter methylation changes, excluding genes affected by both mutations and DNA methylation within the same patient, and also excluding hypermutated cases. We then compared those gene lists across patients to count the number of genes that are mutated in one patient but affected by DNA methylation changes in another patient (Table S6).

Immunohistochemistry

Immunohistochemistry for MIB1 (Ki-67) was performed at the Brain Tumor Research Center, University of California San Francisco, using a Ventana automated immunohistochemical staining processor and the CONFIRM anti-Ki-67 (30-9) Rabbit Monoclonal Primary Antibody (Ventana). Areas of maximal nuclear staining were selected for quantification of labeling index (LI), defined as the number of MIB1 positive cells divided by the total number of cells. At least 1,000 cells were evaluated, and quantification was performed either by manual counting under a light microscope containing an eyepiece micrometer grid or through a semi-automated image analysis approach. Image acquisition was performed using an Olympus BX-41 microscope, 20X objective, and Olympus DP21 digital camera, and analysis was done using Image J (http://imagej.nih.gov/ij/) and the ImmunoRatio plug-in (http://153.1.200.58/sites/default/files/software/immunoratio-plugin/index.html).

SUPPLEMENTAL REFERENCES

Kleinman, C. L., Gerges, N., Papillon-Cavanagh, S., Sin-Chan, P., Pramatarova, A., Quang, D. A., Adoue, V., Busche, S., Caron, M., Djambazian, H., *et al*. (2014). Fusion of TTYH1 with the C19MC microRNA cluster drives expression of a brain-specific DNMT3B isoform in the embryonal brain tumor ETMR. Nat Genet *46*, 39-44.

Krueger, F., and Andrews, S. (2011). Bismark: a flexible aligner and methylation caller for Bisulfite-Seq applications. Bioinformatics (Oxford, England) *27*, 1571-1573.

Smyth, G. K. (2004). Linear models and empirical bayes methods for assessing differential expression in microarray experiments. Statistical applications in genetics and molecular biology *3*, Article3.

Storey, J. D., and Tibshirani, R. (2003). Statistical significance for genomewide studies. Proceedings of the National Academy of Sciences of the United States of America *100*, 9440-9445.

Yu, G., Wang, L. G., Han, Y., and He, Q. Y. (2012). clusterProfiler: an R package for comparing biological themes among gene clusters. Omics : a journal of integrative biology *16*, 284-287.